



Theoretical Investigation on Highly Efficient Quinacridone Derivatives for Green Dopant OLEDs: A DFT Simulation

S. Palanisamy¹, P. Srinivasan², A. David Stephen³, B. Jothi¹, K. Selvaraju^{1*}

¹Department of Physics, Kandaswami Kandari's College, Velur-638182, Namakkal (Dt.) India

²Department of Physics, Chikkaiah Naicker College, Erode-638004, Erode (Dt), India

³Department of Physics, PSG College of Arts and Science, Coimbatore, India

ABSTRACT: The present computational work deals with the Quinacridone green dopant theoretical organic light emitting diode molecule has been carried out with density functional theory by using Gaussian09 package. All the quantum chemical calculations have been performed with HF, B3LYP and B3PW91 functional methods. The structural parameter, bond topological analysis and the corresponding electrostatic and transport properties of the OLED molecule has been calculated. The laplacian of electron density and bond ellipticity of molecule have been studied for various optimized methods. The atomic charges of the molecule for different optimized methods has been analysed with AIM, MPA and NPA charges. The HLG of the molecule are calculated from different optimized basis sets. The HF method value is 8.49 eV. The B3LYP and B3PW91 methods energy values are 3.13 eV and 3.12 eV respectively. These values are most equal to the energy gap obtained from density of states (DOS) spectrum. Hence, the ESP shows that expend of O-atoms and the charge accumulated through Quinacridone OLED molecule. The grateful Quinacridone green dopant derivative molecule is high quantum efficiency, longer lifetime and very useful to industrial organic pigment of these molecules.

KEYWORDS: AIM, DFT, ESP, HLG, OLED.

1. INTRODUCTION

Developing the new concept of this Quinacridone molecule is still challenges for the scientific researcher in computational work. In 1935, it was first synthesized by Quinacridone organic molecule. It is used in the formation of organic pigments [1]. Since 1958, the organic pigment of Quinacridone molecule is used industrially produced by DuPont [2-4]. It has high performance pigment of Quinacridone (QA) organic molecule a common mass produced to industrial organic pigment which discovers a large scale widely used in the exceptional color, weather fastness. Full-color emissive organic materials have attracted significant attention in recent years as key components in the display and lighting devices based on OLEDs [5]. During the past three years, the QA derivatives of electronic devices have been explored. The excellent electrical properties, semiconducting polymers have been attracting extensive in the solution processed organic electronics components such as, organic field-effect transistors (Koezuka et al.), organic photovoltaic, organic solar cells [6] also analysed. In this QA pigment exhibits high electroluminescence quantum efficiency, long lifetime, temporal stability and good thermal properties of the molecule is reported and experimentally values are resulted [7, 8].

In particularly, recent researchers almost used in organic materials have been fabrication of the organic light-emitting devices (OLED) of QA green dopant organic molecules have been attracting for different potential application [9, 10]. Because, it is used as the quantum efficiency of electron and the electron charge carrier also increased from this organic OLED molecule [11-14]. The applications of electronic structure have been analysed for this research studies. In generally, the organic materials are preferred the outstanding their low cost, ease of fine-tuning, solution processability, low toxicity and sufficient flexibility for fabrications of OLED devices [15]. QA pigments are very novel pigments that have many used as industrial paints, printing inks, plastics and textiles etc. [16-18]. QA derivatives are widely investigated for many applications in various fields, but very rarely involved in biological applications. In the present research investigation, QA derivatives organic molecules of functional N-H, O-C and C-C groups are presented from Fig.1. These are the polar group formation of intermolecular hydrogen bonds in the research molecule [19]. Although these functional group effects also break through the conjugation of the QA molecule and thereby consequentially changes the HOMO-LUMO energy gap distances. The spatial hybridization shapes of the molecular frontier orbitals and their energies [20] are calculated. Also, from the density of states (DOS) of this molecule, we obtain the energy gap, which

describes its electric properties of the molecule. Finally, we calculate from HLG distance of the QA organic molecule. The electrostatic potential (ESP) of charged region also calculated and classified strong electronegative and positive regions present in the QA molecule. On the other hand of this molecule, both potential occur only O-atoms through this molecule. Because, this difference attributed through the N-atoms surrounding connected only C and H atoms. The aim of our research investigation, the highly efficient green dopant QA organic light emitting diode molecule deals with computational details, structural aspects, charge density distribution, laplacian of electron density, bond ellipticity, atomic charges, molecular orbital analysis and their energies also studied. Finally, the molecular electrostatic potential (ESP) has been analysed for this research articles.

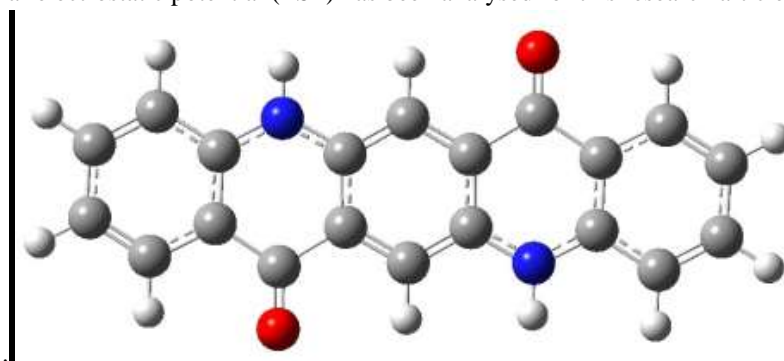


Figure.1. Chemical structure of Quinacridone molecule.

2. COMPUTATIONAL DETAILS

The Quinacridone OLED molecule has been carried out with density functional theory (DFT) with the different basis sets HF, B3LYP and B3PW91 by using Gaussian09 program [21-23]. Figure.2 illustrates that all the optimized geometry was performed via Berny algorithm in redundant internal co-ordinates. The threshold convergence for maximum force, root mean square (RMS) force, maximum displacement and root mean square (RMS) displacement are 0.00045, 0.0003, 0.001 and 0.0012 au respectively. The self-consistency of non-interactive wave function was performed with a requested convergence on the density matrix of 10^{-8} and 10^{-6} for the RMS and maximum density matrix error between the iterations [24]. By using Bader's theory of "Atoms in Molecules" (AIM) the bond topological and the electrostatic properties have been calculated from the EXT94b routine incorporated to the AIMPAC software [25]. The atomic charges, such as AIM, MPA and NPA are calculated from the AIMALL software package. The deformation density and Laplacian of electron density maps are calculated from the *wfn2plots* and *XD package* [26]. An Isosurface region of the molecule has been plotted by using Gview programme package [27]. The GaussSum program [28] has been used to determine the density of states (DOS) of the QA molecule for different methods of optimization.

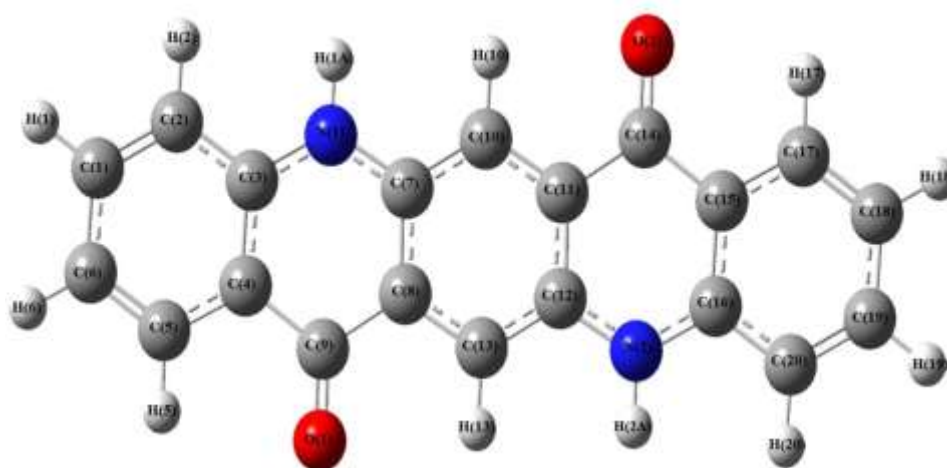
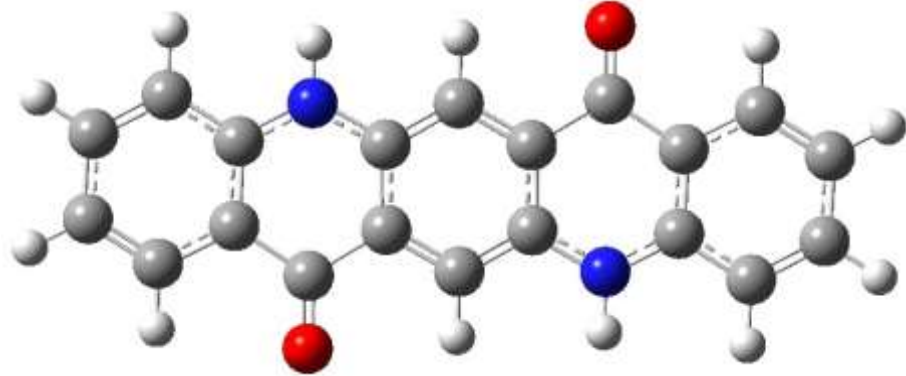
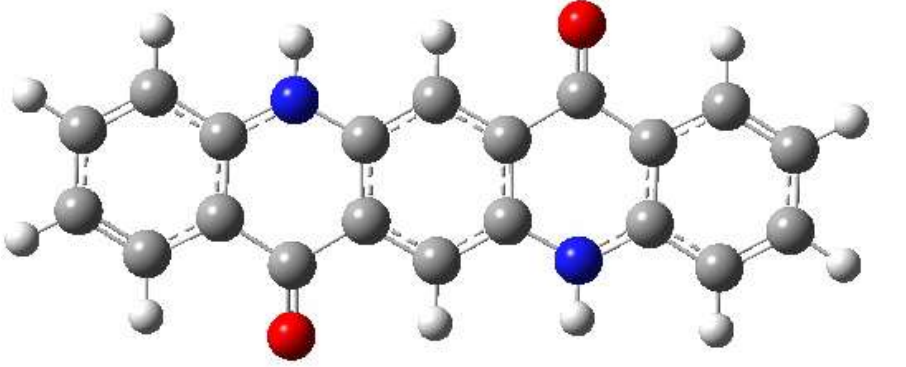


Figure. 2. Optimized geometry of Quinacridone molecule.

3. RESULTS AND DISCUSSION

3.1. Structural aspects

Quinacridone (QA) is an outstanding with the combined computational and experimental approach in the OLED organic molecules for academic research studies. It have become an extremely used in the synthesis has been developed by many researches. In this dihydropyridin-4(3H)-one compound are extensively used in the effective of all type of research studies [29]. Most of these studies are synthesised by low yields, low selectivity and the availability of materials for this compounds [30, 31]. In the present research study of Quinacridone molecule has three aromatic rings and two compound of dihydropyridin-4(3H)-one are combined through this optimized structure. The dihydropyridin-4(3H)-one rings in N-atom indicates blue colors and O-atom indicates red colors for this optimized structure. Nowadays, a most researcher is widely used in the theoretical studies of different optimized methods. Such as, HF, B3LYP and B3PW91 methods has been used to calculate the structural parameters, charge density distribution and the molecular orbitals of Quinacridone OLED molecule. The bond distance extents of the HF methods are found to be smaller than the other two methods of B3LYP and B3PW91 respectively. Fig.3. depicts that the Quinacridone molecule has been optimized by different methods. In the present computational research of Quinacridone OLED molecule, the aromatic ring-I in the C–C bond lengths of the molecule are optimized form HF methods are vary from ~1.369 Å to 1.401 Å. These bond distances (ring-II) are increases form 1.399 Å to 1.487 Å. However, the C–C bond distances (rings-III, IV and V) are increases from 1.369 Å to 1.487 Å respectively. The Quinacridone molecule has been optimized with B3LYP using the basis set 6-311G** and all the C–C bonds are increases from 1.381 Å to 1.484 Å. Similarly, the aromatic rings of the C–C bond distance of these optimized B3PW91 methods are increases from 1.379 Å to 1.480 Å. The maximum observed variation for all C–C bonds are 0.018 Å.

Methods	Optimized geometry
HF/ 6-311G(d,p)	
B3LYP/ 6-311G(d,p)	

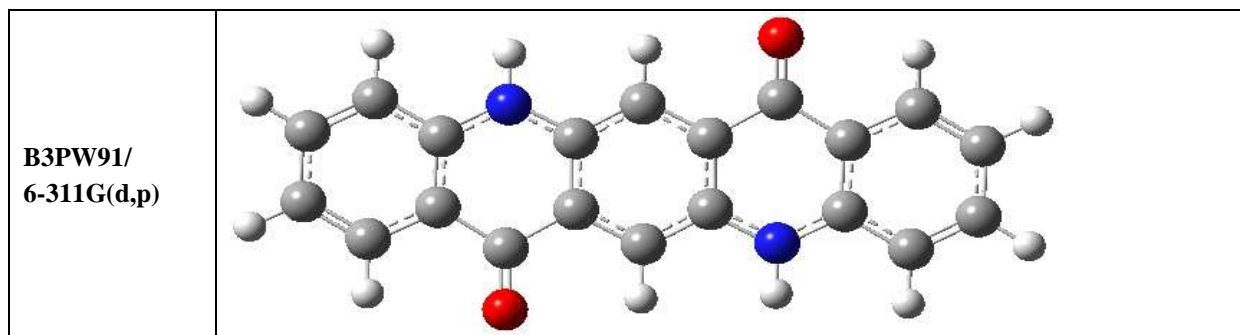


Figure.3. Optimized geometry of Quinacridone molecule at HF, B3LYP and B3PW91 levels.

Especially, the N–C bond distance of the molecule is slightly modified from ~ 1.368 Å to 1.381 Å for HF method. Notably, the N–C bonds of the molecule are lightly increases form 1.376 Å to 1.383 Å for B3LYP methods. Finally, the molecule has been optimized with B3PW91 method by using the basis set of 6-311G**. These bonds are barely modified from 1.372 Å to 1.378 Å respectively. The main focuses on O–C bond distances are calculated. It is found to be equal (1.197 Å, 1.226 Å and 1.224 Å) for all the optimized methods HF, B3LYP and B3PW91 respectively.

The C–H bond distance of QA molecule for HF method range slightly varies from ~ 1.074 Å to 1.076 Å. In the other optimized method of B3LYP, these bond distances are lightly differ from ~ 1.083 Å to ~ 1.085 Å respectively. Finally, the B3PW91 optimized method, the C–H bond distance of the molecule are slightly changes from ~ 1.084 Å to ~ 1.086 Å respectively. The maximum observed variation for all the optimized method is ~ 0.02 Å. Likewise, the bond lengths of N–H bond distance are equal for all the optimized methods (HF= 0.992 Å, B3LYP= 1.008 Å and B3PW91= 1.008 Å). Table.1 represents the bond lengths of the Quinacridone molecule at HF, B3LYP and B3PW91 methods of different optimized levels.

The calculated values of C–C–C bond angles are increasing from 115.4° to 121.2° by using HF method. In additional two different optimized methods (B3LYP and B3PW91), the C–C–C bonds are increases from $\sim 115.3^\circ$ to $\sim 121.1^\circ$ respectively. The bond lengths of C–C–H bonds are almost same value for all the optimized methods. However, the N–C–C bond angles of the molecule are calculated. These values are increasing from $\sim 119.9^\circ$ to $\sim 121^\circ$ in the HF optimized method. Another two optimized methods of (B3LYP and B3PW91) this molecule, these (N–C–C) bonds are varied from $\sim 119.5^\circ$ to $\sim 121.1^\circ$ compared with HF methods. All the same processes of the Quinacridone OLED molecule, the bond angles of O–C–C bonds are altered ($\sim 121.6^\circ$ and $\sim 123^\circ$). Furthermore, the C–N–C bonds of this research investigation slightly increases from 123.1° to 123.4° for all the refine methods. In the same way, the C–N–H bonds are slightly vary from 118.1° to 118.6° for all the optimized methods. Table-2 shows that the selected bond angles of the Quinacridone OLED molecule are presented and compared with different optimized methods.

Table-1 Bond lengths of the Quinacridone OLED molecule at HF, B3LYP and B3PW91 levels.

Bonds	HF/ 6-311G**	B3LYP/ 6-311G**	B3PW91/ 6-311G**
Ring-I			
C(1)-C(2)	1.369	1.382	1.380
C(1)-C(6)	1.400	1.405	1.402
C(2)-C(3)	1.404	1.408	1.406
C(3)-C(4)	1.394	1.412	1.410
C(4)-C(5)	1.401	1.405	1.403
C(5)-C(6)	1.369	1.381	1.379
Ring-II			
C(7)-C(8)	1.399	1.417	1.414
C(8)-C(9)	1.487	1.484	1.480



C(9)-C(4)	1.472	1.474	1.470
Ring-III			
C(7)-C(10)	1.384	1.394	1.392
C(10)-C(11)	1.383	1.392	1.389
C(11)-C(12)	1.399	1.417	1.414
C(12)-C(13)	1.384	1.394	1.392
C(13)-C(8)	1.383	1.392	1.389
Ring-IV			
C(11)-C(14)	1.487	1.484	1.480
C(14)-C(15)	1.472	1.474	1.470
C(15)-C(16)	1.394	1.412	1.410
Ring-V			
C(15)-C(17)	1.401	1.405	1.403
C(16)-C(20)	1.404	1.408	1.406
C(17)-C(18)	1.369	1.381	1.379
C(18)-C(19)	1.400	1.405	1.402
C(19)-C(20)	1.369	1.382	1.380
N-C Bonds			
N(1)-C(3)	1.368	1.376	1.372
N(1)-C(7)	1.381	1.383	1.378
N(2)-C(12)	1.381	1.383	1.378
N(2)-C(16)	1.368	1.376	1.372
O-C Bonds			
O(1)-C(9)	1.197	1.226	1.224
O(2)-C(14)	1.197	1.226	1.224
C-H Bonds			
C(1)-H(1)	1.076	1.084	1.085
C(2)-H(2)	1.076	1.085	1.086
C(5)-H(5)	1.074	1.083	1.084
C(6)-H(6)	1.074	1.083	1.084
C(10)-H(10)	1.074	1.085	1.086
C(13)-H(13)	1.074	1.085	1.086
C(17)-H(17)	1.074	1.083	1.084
C(18)-H(18)	1.074	1.083	1.084
C(19)-H(19)	1.076	1.084	1.085
C(20)-H(20)	1.076	1.085	1.086
N-H Bonds			
N(1)-H(1A)	0.992	1.008	1.008
N(2)-H(2A)	0.992	1.008	1.008



Table-2 Bond angles (°) the Quinacridone OLED molecule at HF, B3LYP and B3PW91 levels.

Bonds	HF/ 6-311G**	B3LYP/ 6-311G**	B3PW91/ 6-311G**
C-C-C Bonds			
C(1)-C(2)-C(3)	119.8	119.9	119.9
C(1)-C(6)-C(5)	119.0	119.4	119.3
C(3)-C(4)-C(9)	120.7	120.9	121.0
C(4)-C(3)-C(2)	119.4	119.6	119.6
C(4)-C(9)-C(8)	115.4	115.4	115.3
C(5)-C(4)-C(3)	119.4	119.1	119.1
C(5)-C(4)-C(9)	119.9	120.0	119.9
C(6)-C(1)-C(2)	121.2	120.9	120.9
C(6)-C(5)-C(4)	121.1	121.1	121.1
C(7)-C(8)-C(13)	120.2	119.7	119.9
C(7)-C(10)-C(11)	120.7	120.8	120.8
C(8)-C(7)-C(10)	119.1	119.5	119.4
C(8)-C(13)-C(12)	120.7	120.8	120.8
C(9)-C(8)-C(7)	120.4	120.8	120.8
C(9)-C(8)-C(13)	119.4	119.5	119.3
C(10)-C(11)-C(14)	119.4	119.5	119.3
C(11)-C(14)-C(15)	115.4	115.4	115.3
C(12)-C(11)-C(10)	120.2	119.7	119.9
C(12)-C(11)-C(14)	120.4	120.8	120.8
C(13)-C(12)-C(11)	119.1	119.5	119.4
C(14)-C(15)-C(17)	119.9	120.0	119.9
C(15)-C(16)-C(20)	119.4	119.6	119.6
C(15)-C(17)-C(18)	121.1	121.1	121.1
C(16)-C(15)-C(14)	120.7	120.9	121.0
C(16)-C(15)-C(17)	119.4	119.1	119.1
C(16)-C(20)-C(19)	119.8	119.9	119.9
C(19)-C(18)-C(17)	119.0	119.4	119.3
C(20)-C(19)-C(18)	121.2	120.9	120.9
N-C-C Bonds			
N(1)-C(3)-C(2)	120.1	120.4	120.4
N(1)-C(3)-C(4)	120.5	120.0	120.0
N(1)-C(7)-C(8)	119.9	119.5	119.5
N(1)-C(7)-C(10)	121.0	121.1	121.1
N(2)-C(12)-C(11)	119.9	119.5	119.5
N(2)-C(12)-C(13)	121.0	121.1	121.1
N(2)-C(16)-C(15)	120.5	120.0	120.0



N(2)-C(16)-C(20)	120.1	120.4	120.4
O-C-C Bonds			
O(1)-C(9)-C(4)	123.0	122.8	122.9
O(1)-C(9)-C(8)	121.6	121.7	121.8
O(2)-C(14)-C(11)	121.6	121.7	121.8
O(2)-C(14)-C(15)	123.0	122.8	122.9
C-N-C Bonds			
C(3)-N(1)-C(7)	123.1	123.4	123.4
C(12)-N(2)-C(16)	123.1	123.4	123.4
C-C-H Bonds			
C(6)-C(1)-H(1)	119.7	119.9	119.9
C(2)-C(1)-H(1)	119.1	119.3	119.2
C(1)-C(2)-H(2)	120.5	120.5	120.5
C(3)-C(2)-H(2)	119.6	119.6	119.6
C(6)-C(5)-H(5)	121.3	121.8	121.9
C(4)-C(5)-H(5)	117.6	117.2	117.1
C(1)-C(6)-H(6)	120.3	120.1	120.1
C(5)-C(6)-H(6)	120.8	120.5	120.5
C(7)-C(10)-H(10)	121.2	121.7	121.9
C(11)-C(10)-H(10)	118.1	117.5	117.3
C(8)-C(13)-H(13)	118.1	117.5	117.3
C(12)-C(13)-H(13)	121.2	121.7	121.9
C(15)-C(17)-H(17)	117.6	117.2	117.1
C(18)-C(17)-H(17)	121.3	121.8	121.9
C(19)-C(18)-H(18)	120.3	120.1	120.1
C(17)-C(18)-H(18)	120.8	120.5	120.5
C(20)-C(19)-H(19)	119.1	119.3	119.2
C(18)-C(19)-H(19)	119.7	119.9	119.9
C(16)-C(20)-H(20)	119.6	119.6	119.6
C(19)-C(20)-H(20)	120.5	120.5	120.5
C-N-H Bonds			
C(3)-N(1)-H(1A)	118.6	118.5	118.5
C(7)-N(1)-H(1A)	118.3	118.1	118.1
C(12)-N(2)-H(2A)	118.3	118.1	118.1
C(16)-N(2)-H(2A)	118.6	118.5	118.5

3.2 Charge density distribution

The present research investigation on aims to explore the quantum topological features of the charge density distribution, laplacian of electron density and bond ellipticity also calculated (Table-3). The bond critical points (3, -1) in the Quinacridone OLED molecule are found to be all the chemical bonds of this molecule. From fig.4 (a)-(c) shows that the Quinacridone molecule is plotted in deformation density maps. The HF methods represent the high electron density (ring-I) at bond critical points [$\rho_{BCP(r)}^A$]



of the C–C bond distance of the molecules are decreases from $2.254 \text{ e}\text{\AA}^{-3}$ to $2.130 \text{ e}\text{\AA}^{-3}$. In the same bonds (C–C) of Quinacridone molecule are decreases from $2.136 \text{ e}\text{\AA}^{-3}$ to $2.029 \text{ e}\text{\AA}^{-3}$ for B3LYP method. The eventual optimized method of B3PW91, the C–C bond distances are slightly decreases form $2.134 \text{ e}\text{\AA}^{-3}$ to $2.031 \text{ e}\text{\AA}^{-3}$. From ring-I the maximum observed variations in all C–C bonds are $\sim 0.225 \text{ e}\text{\AA}^{-3}$ for all optimized methods. Similarly, the Quinacridone OLED molecule in the ring-II of C–C bonds are altered. These values are ($2.159 \text{ e}\text{\AA}^{-3}$ to $1.908 \text{ e}\text{\AA}^{-3}$) for HF method. The B3LYP and B3PW91 optimized methods of (ring-II) C–C bonds are largely decreases from $2.018 \text{ e}\text{\AA}^{-3}$ to $1.818 \text{ e}\text{\AA}^{-3}$ respectively. On compared with HF method, the C–C bond distances are also decreases from B3LYP and B3PW91 methods. The maximum observed variation for all optimized levels in the C–C bonds are $\sim 0.341 \text{ e}\text{\AA}^{-3}$. These maximum observed values are high with compared to ring-I of the Quinacridone OLED molecule. However, the aromatic ring-III and ring-V of C–C bonds are increases from ~ 2.017 to $\sim 2.254 \text{ e}\text{\AA}^{-3}$ for all different optimized methods. Finally, the C–C bonds in the molecule of ring-IV are found to be not equal ($\sim 2.166 \text{ e}\text{\AA}^{-3}$ to $\sim 1.818 \text{ e}\text{\AA}^{-3}$) for all the optimized methods. The maximum observed for C–C bonds are $\sim 0.348 \text{ e}\text{\AA}^{-3}$. The bond critical points of C–H bonds of the molecule are decreases from $\sim 2.015 \text{ e}\text{\AA}^{-3}$ to $\sim 1.879 \text{ e}\text{\AA}^{-3}$ for all the optimized methods. The important bonds of Quinacridone molecule in N–C bonds are differing from HF method. These values are decreases from $\sim 2.103 \text{ e}\text{\AA}^{-3}$ to $2.048 \text{ e}\text{\AA}^{-3}$. Alternative two optimized methods, these bonds are little changed of ring-II and ring-IV of the molecule. These values are varying from $\sim 2.059 \text{ e}\text{\AA}^{-3}$ to $2.022 \text{ e}\text{\AA}^{-3}$ respectively [32]. The studies of N–H bond distances are almost same value in all optimized methods. These bond values are varied from $\sim 2.431 \text{ e}\text{\AA}^{-3}$ to $\sim 2.309 \text{ e}\text{\AA}^{-3}$. Likewise, O–C bond distance of HF, B3LYP and B3PW91 optimization methods are large decreases from $\sim 2.858 \text{ e}\text{\AA}^{-3}$ to $\sim 2.681 \text{ e}\text{\AA}^{-3}$ respectively. The maximum observed variation for all optimized methods are $\sim 0.177 \text{ e}\text{\AA}^{-3}$. In future this study, the bond critical point was located almost equally distance from N–C bonds of the Quinacridone OLED molecule.

3.3 Laplacian of Electron density

Fig.5 (a)-(c) represents the Laplacian of electron density [$\nabla^2 \rho_{\text{BCP}(r)}$] of Quinacridone OLED molecule at HF, B3LYP and B3PW91 different optimized levels. The present computational investigation deals with the Laplacian of the electron density of the Quinacridone OLED molecule about the nature of all the bonds are calculated [33, 34]. From this research articles, the optimized methods (HF, B3LYP and B3PW91) of the N–C bond distance of the molecule are (negative values) separately increasing from $-15.272 \text{ e}\text{\AA}^{-5}$ to $-18.955 \text{ e}\text{\AA}^{-5}$. The N–H bond distance are as well as negative value. These values are increasing from $-39.774 \text{ e}\text{\AA}^{-5}$ to $-47.953 \text{ e}\text{\AA}^{-5}$. However, the O–C bond distances are very extremely increasing from $-4.750 \text{ e}\text{\AA}^{-5}$ to $5.050 \text{ e}\text{\AA}^{-5}$ for entire optimized methods. The Laplacian of electron density of C–C bond distance are along only negative value for all the optimized methods. These bond distances are increasing (negative value) from $-16.272 \text{ e}\text{\AA}^{-5}$ to $-25.945 \text{ e}\text{\AA}^{-5}$ respectively. Particularly, the C–H bond distance are increasing (negative values) from $-22.738 \text{ e}\text{\AA}^{-5}$ to $-27.411 \text{ e}\text{\AA}^{-5}$ for all optimized methods. Table-3 shows that the Laplacian of electron density was calculated and tabulated.

3.4 Bond ellipticity

The anisotropy of electron density distribution at bcp also calculated by using the bond ellipticity (ϵ). In generally, it is defined as, to measuring the anisotropy of the electron distribution at r_p . It is well defined, $\epsilon = (\lambda_1 / \lambda_2) - 1$. Here, λ_1 and λ_2 are the negative eigen value of Hessian matrix [35, 36]. The positive value specifies contraction of electron density. The maximum bond ellipticity large values are signifying and hence, due to the intermolecular of these bonding characters are Pi bonds interaction of these studies. The N–C bond distances are (negative) increases from -14.518 to -15.724 for all the optimized methods. However, the N–H bonds distance of the molecule (negative values) are increasing from -31.432 to -34.381 . In addition, the bond distance of O–C bonds (negative value) are found to be unequal. These bonds are increasing from -23.828 to -28.565 respectively. The mean values of C–C bond distances are vary from -13.289 to -17.425 for all the optimized methods (Table-3). The maximum observed variation for these bonds are ~ 4.14 . Furthermore, the C–H bond distances are found to be unequal for all optimization methods. These bond distances are varied from -17.732 to -19.453 .

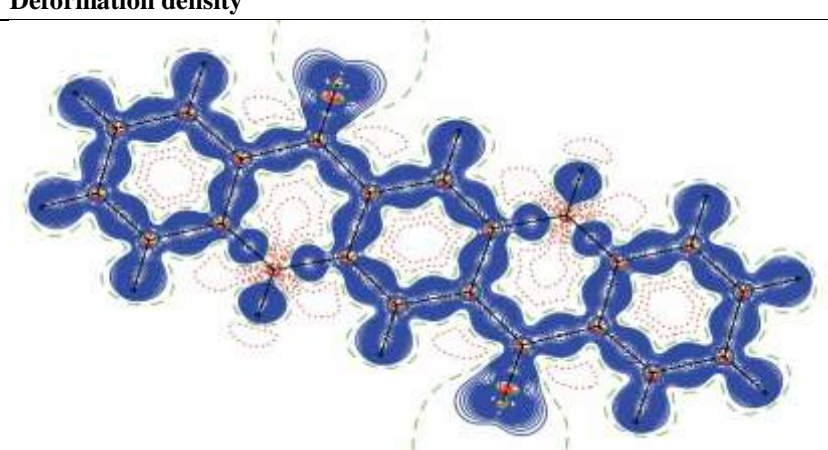
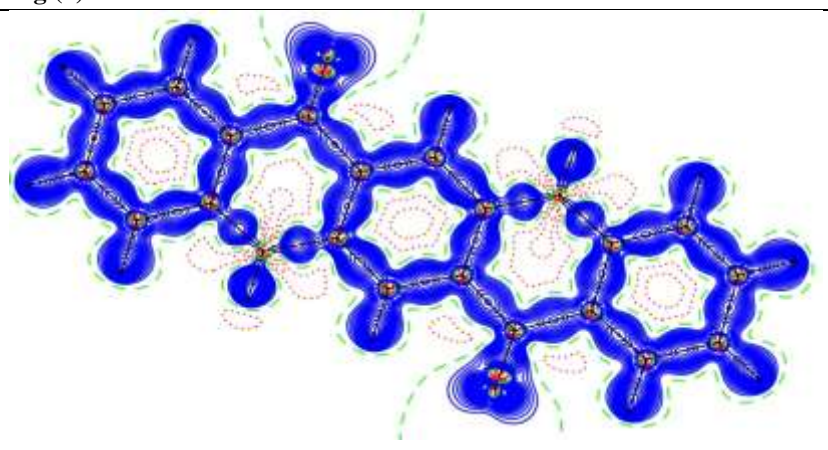
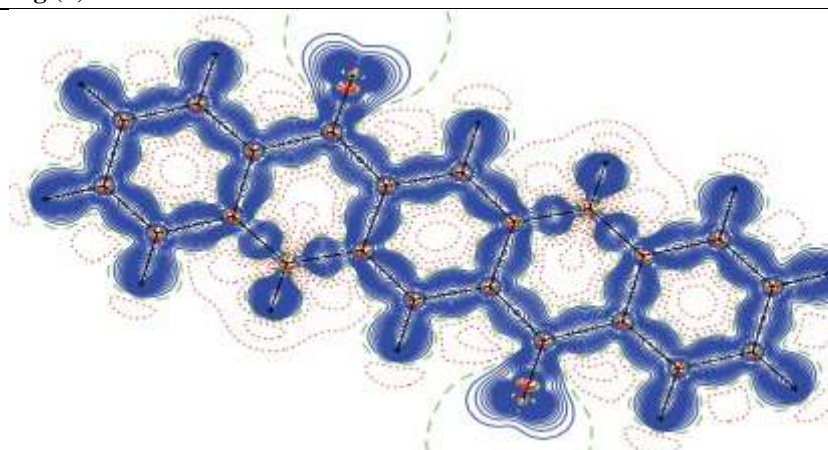
Methods	Deformation density
HF/ 6-311G**	 <p>Fig.(a)</p>
B3LYP/ 6-311G**	 <p>Fig.(b)</p>
B3PW91/ 6- 311G**	 <p>Fig.(c)</p>

Figure.4 (a)-(c) Shows the deformation density maps of Quinacridone molecule at HF, B3LYP and B3PW91 level. Solid lines: Positive contours. Dotted lines: Negative contours and Dashed lines: zero contours are drawn at $\pm 0.05 \text{ e}\text{\AA}^{-3}$ intervals.

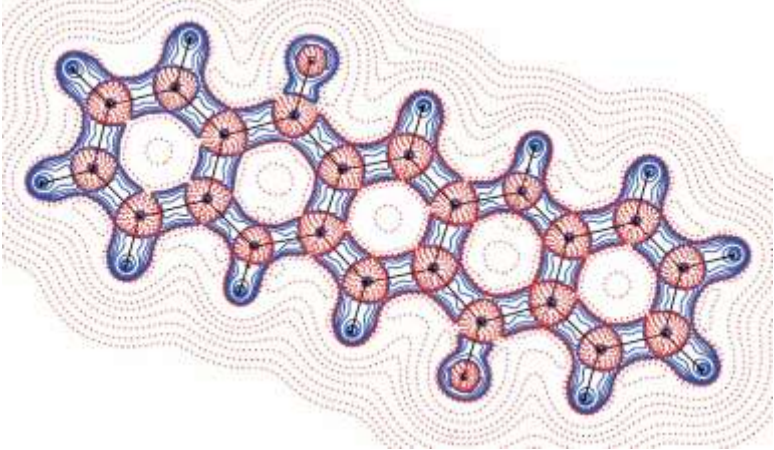
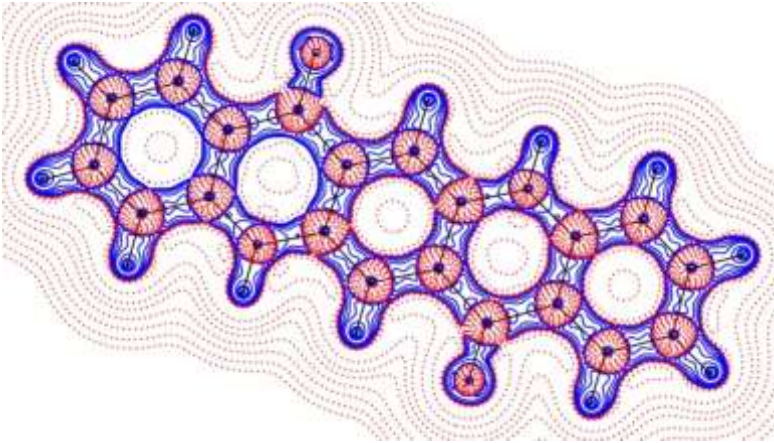
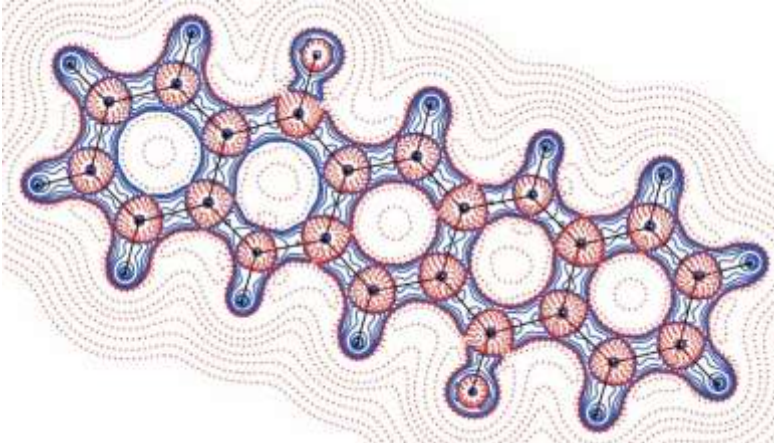
Methods	Laplacian of electron density
HF/6-311G**	 <p data-bbox="432 898 507 927">Fig.(a)</p>
B3LYP/6-311G**	 <p data-bbox="432 1413 507 1442">Fig.(b)</p>
B3PW91/6-311G**	 <p data-bbox="432 1928 507 1957">Fig.(c)</p>

Figure.5 (a)-(c). The Laplacian of electron density of Quinacridone molecule at HF, B3LYP and B3PW91 methods. The contours are drawn in logarithmic scale, $3.0 \times 2^N e \text{Å}^{-5}$.



Table.3. Bond topological properties of Quinacridone molecule at HF, B3LYP and B3PW91 methods.

Bonds	$\rho_{\text{BCP}(r)}^a$	$\nabla^2\rho_{\text{BCP}(r)}^b$	ϵ^c	λ_1^d	λ_2^d	λ_3^d	d_1	d_2	D
Ring-I									
C(1)-C(2)	2.246	-25.657	-17.376	-13.575	5.293	0.280	0.681	0.689	1.369
	2.127	-21.390	-15.999	-12.987	7.596	0.232	0.694	0.688	1.382
	2.125	-21.343	-15.799	-12.813	7.269	0.233	0.686	0.693	1.380
C(1)-C(6)	2.138	-24.018	-16.235	-13.489	5.706	0.204	0.725	0.675	1.400
	2.046	-20.145	-15.191	-12.861	7.906	0.181	0.713	0.692	1.405
	2.047	-20.157	-15.025	-12.715	7.582	0.182	0.691	0.712	1.402
C(2)-C(3)	2.132	-24.040	-16.288	-13.234	5.481	0.231	0.754	0.650	1.404
	2.040	-19.981	-15.248	-12.627	7.895	0.208	0.732	0.676	1.408
	2.041	-19.990	-15.084	-12.483	7.577	0.208	0.674	0.732	1.406
C(3)-C(4)	2.166	-24.418	-16.601	-13.057	5.240	0.271	0.753	0.642	1.395
	2.029	-19.669	-15.086	-12.492	7.909	0.208	0.736	0.676	1.413
	2.031	-19.725	-14.942	-12.373	7.590	0.208	0.675	0.735	1.410
C(4)-C(5)	2.130	-23.650	-16.109	-13.382	5.841	0.204	0.703	0.698	1.401
	2.044	-20.012	-15.110	-12.827	7.925	0.178	0.709	0.696	1.405
	2.046	-20.050	-14.960	-12.694	7.604	0.178	0.695	0.708	1.403
C(5)-C(6)	2.254	-25.945	-17.425	-13.746	5.226	0.268	0.703	0.665	1.369
	2.136	-21.642	-16.052	-13.187	7.597	0.217	0.696	0.685	1.381
	2.134	-21.592	-15.851	-13.011	7.271	0.218	0.684	0.695	1.379
Ring-II									
C(7)-C(8)	2.159	-24.278	-16.590	-13.355	5.667	0.242	0.731	0.668	1.399
	2.017	-19.521	-15.004	-12.567	8.049	0.194	0.729	0.688	1.417
	2.018	-19.565	-14.858	-12.444	7.736	0.194	0.686	0.728	1.414
C(8)-C(9)	1.908	-20.305	-14.362	-13.012	7.069	0.104	0.748	0.739	1.487
	1.818	-16.272	-13.335	-11.961	9.024	0.115	0.749	0.735	1.484
	1.826	-16.461	-13.289	-11.911	8.739	0.116	0.732	0.748	1.480
C(9)-C(4)	1.946	-20.845	-14.746	-12.983	6.884	0.136	0.748	0.724	1.472
	1.847	-16.727	-13.620	-12.038	8.931	0.131	0.738	0.736	1.474
	1.855	-16.902	-13.565	-11.979	8.642	0.132	0.735	0.735	1.470
Ring-III									
C(7)-C(10)	2.205	-25.193	-17.027	-13.542	5.376	0.257	0.655	0.730	1.384
	2.092	-20.825	-15.710	-12.853	7.738	0.222	0.673	0.721	1.394
	2.090	-20.797	-15.524	-12.691	7.418	0.223	0.721	0.671	1.392
C(10)-C(11)	2.189	-24.565	-16.704	-13.406	5.545	0.246	0.695	0.688	1.383
	2.087	-20.645	-15.530	-12.845	7.730	0.209	0.698	0.694	1.392
	2.088	-20.660	-15.366	-12.698	7.404	0.210	0.692	0.697	1.389
C(11)-C(12)	2.159	-24.278	-16.590	-13.355	5.667	0.242	0.668	0.731	1.399
	2.017	-19.522	-15.004	-12.567	8.049	0.194	0.688	0.729	1.417



	2.018	-19.565	-14.858	-12.444	7.736	0.194	0.728	0.686	1.414
C(12)-C(13)	2.205	-25.193	-17.027	-13.542	5.376	0.257	0.730	0.655	1.384
	2.092	-20.825	-15.710	-12.853	7.738	0.222	0.721	0.673	1.394
	2.090	-20.797	-15.524	-12.691	7.418	0.223	0.671	0.721	1.392
C(13)-C(8)	2.189	-24.565	-16.704	-13.406	5.545	0.246	0.688	0.695	1.383
	2.087	-20.646	-15.530	-12.845	7.730	0.209	0.694	0.698	1.392
	2.088	-20.660	-15.366	-12.698	7.404	0.210	0.697	0.692	1.389
Ring-IV									
C(11)-C(14)	1.908	-20.305	-14.362	-13.012	7.069	0.104	0.739	0.748	1.487
	1.818	-16.272	-13.335	-11.961	9.024	0.115	0.735	0.749	1.484
	1.826	-16.461	-13.289	-11.911	8.739	0.116	0.748	0.732	1.480
C(14)-C(15)	1.946	-20.845	-14.746	-12.983	6.884	0.136	0.724	0.748	1.472
	1.847	-16.727	-13.620	-12.038	8.931	0.131	0.736	0.738	1.474
	1.855	-16.902	-13.565	-11.979	8.642	0.132	0.735	0.735	1.470
C(15)-C(16)	2.166	-24.418	-16.601	-13.057	5.240	0.271	0.642	0.753	1.395
	2.029	-19.670	-15.086	-12.493	7.909	0.208	0.676	0.736	1.413
	2.031	-19.725	-14.942	-12.373	7.590	0.208	0.735	0.675	1.410
Ring-V									
C(15)-C(17)	2.130	-23.650	-16.109	-13.382	5.841	0.204	0.698	0.703	1.401
	2.044	-20.011	-15.110	-12.827	7.925	0.178	0.696	0.709	1.405
	2.046	-20.050	-14.960	-12.694	7.604	0.178	0.708	0.695	1.403
C(16)-C(20)	2.132	-24.040	-16.288	-13.234	5.481	0.231	0.650	0.754	1.404
	2.040	-19.981	-15.248	-12.628	7.895	0.208	0.676	0.732	1.408
	2.041	-19.990	-15.084	-12.483	7.577	0.208	0.732	0.674	1.406
C(17)-C(18)	2.254	-25.945	-17.425	-13.746	5.226	0.268	0.665	0.703	1.369
	2.136	-21.642	-16.052	-13.187	7.597	0.217	0.685	0.696	1.381
	2.134	-21.592	-15.851	-13.011	7.271	0.218	0.695	0.684	1.379
C(18)-C(19)	2.138	-24.018	-16.235	-13.489	5.706	0.204	0.675	0.725	1.400
	2.046	-20.145	-15.190	-12.861	7.906	0.181	0.692	0.713	1.405
	2.047	-20.157	-15.025	-12.715	7.582	0.182	0.712	0.691	1.402
C(19)-C(20)	2.246	-25.657	-17.376	-13.575	5.293	0.280	0.689	0.681	1.369
	2.127	-21.390	-15.999	-12.987	7.596	0.232	0.688	0.694	1.382
	2.125	-21.343	-15.799	-12.813	7.269	0.233	0.693	0.686	1.380
N-C Bonds									
N(1)-C(3)	2.103	-15.461	-15.724	-15.516	15.779	0.013	0.911	0.457	1.368
	2.047	-18.955	-14.785	-13.645	9.475	0.084	0.876	0.500	1.376
	2.059	-18.236	-14.674	-13.616	10.055	0.078	0.492	0.879	1.372
N(1)-C(7)	2.048	-15.272	-14.973	-14.674	14.375	0.020	0.462	0.919	1.381
	2.022	-18.924	-14.614	-13.313	9.003	0.098	0.505	0.877	1.383
	2.035	-18.300	-14.518	-13.287	9.505	0.093	0.881	0.497	1.378



N(2)-C(12)	2.048	-15.272	-14.973	-14.674	14.375	0.020	0.919	0.462	1.381
	2.022	-18.924	-14.614	-13.313	9.004	0.098	0.877	0.505	1.383
	2.035	-18.300	-14.518	-13.287	9.505	0.093	0.497	0.881	1.378
N(2)-C(16)	2.103	-15.461	-15.724	-15.516	15.779	0.013	0.457	0.911	1.368
	2.047	-18.955	-14.785	-13.645	9.475	0.084	0.500	0.876	1.376
	2.059	-18.236	-14.674	-13.616	10.055	0.078	0.879	0.492	1.372
O-C Bonds									
O(1)-C(9)	2.858	5.050	-28.565	-27.722	61.337	0.030	0.398	0.799	1.197
	2.681	-4.750	-23.877	-22.934	42.061	0.041	0.419	0.807	1.226
	2.685	-3.341	-23.828	-22.892	43.378	0.041	0.807	0.417	1.224
O(2)-C(14)	2.858	5.050	-28.565	-27.722	61.337	0.030	0.799	0.398	1.197
	2.681	-4.751	-23.877	-22.933	42.058	0.041	0.807	0.419	1.226
	2.685	-3.341	-23.828	-22.892	43.379	0.041	0.417	0.807	1.224
C-H Bonds									
C(1)-H(1)	1.993	-26.849	-18.793	-18.667	10.611	0.007	0.685	0.375	1.059
	1.909	-23.552	-18.159	-17.940	12.547	0.012	0.694	0.375	1.070
	1.903	-23.447	-17.975	-17.769	12.296	0.012	0.373	0.697	1.070
C(2)-H(2)	1.961	-25.842	-18.250	-17.645	10.053	0.034	0.381	0.678	1.059
	1.885	-22.846	-17.732	-17.272	12.158	0.027	0.380	0.691	1.071
	1.879	-22.738	-17.547	-17.105	11.914	0.026	0.694	0.378	1.071
C(5)-H(5)	2.015	-27.411	-19.453	-19.313	11.355	0.007	0.694	0.363	1.056
	1.925	-23.987	-18.670	-18.467	13.150	0.011	0.702	0.366	1.068
	1.917	-23.856	-18.464	-18.271	12.879	0.011	0.364	0.705	1.069
C(6)-H(6)	1.979	-26.322	-18.609	-18.060	10.347	0.030	0.680	0.377	1.057
	1.905	-23.370	-18.110	-17.704	12.444	0.023	0.692	0.376	1.069
	1.899	-23.269	-17.927	-17.538	12.196	0.022	0.374	0.695	1.069
C(10)-H(10)	1.994	-26.729	-19.097	-18.723	11.091	0.020	0.365	0.692	1.057
	1.904	-23.390	-18.329	-17.984	12.923	0.019	0.368	0.702	1.070
	1.896	-23.256	-18.122	-17.792	12.659	0.019	0.705	0.366	1.071
C(13)-H(13)	1.994	-26.729	-19.097	-18.723	11.091	0.020	0.692	0.365	1.057
	1.904	-23.390	-18.329	-17.984	12.923	0.019	0.702	0.368	1.070
	1.896	-23.256	-18.122	-17.792	12.659	0.019	0.366	0.705	1.071
C(17)-H(17)	2.015	-27.411	-19.453	-19.313	11.355	0.007	0.363	0.694	1.056
	1.925	-23.987	-18.670	-18.467	13.150	0.011	0.366	0.702	1.068
	1.917	-23.856	-18.464	-18.271	12.879	0.011	0.705	0.364	1.069
C(18)-H(18)	1.979	-26.322	-18.609	-18.060	10.347	0.030	0.377	0.680	1.057
	1.905	-23.370	-18.110	-17.704	12.444	0.023	0.376	0.692	1.069
	1.899	-23.269	-17.927	-17.538	12.196	0.022	0.695	0.374	1.069
C(19)-H(19)	1.993	-26.849	-18.793	-18.667	10.611	0.007	0.375	0.685	1.059
	1.909	-23.552	-18.159	-17.940	12.547	0.012	0.375	0.694	1.070



	1.903	-23.447	-17.975	-17.769	12.296	0.012	0.697	0.373	1.070
C(20)-H(20)	1.961	-25.842	-18.250	-17.645	10.053	0.034	0.678	0.381	1.059
	1.885	-22.846	-17.732	-17.272	12.158	0.027	0.691	0.380	1.071
	1.879	-22.738	-17.547	-17.105	11.914	0.026	0.378	0.694	1.071
N-H Bonds									
N(1)-H(1A)	2.431	-47.953	-34.381	-32.303	18.731	0.064	0.228	0.742	0.969
	2.309	-39.774	-31.432	-29.771	21.429	0.056	0.248	0.740	0.989
	2.312	-40.468	-31.537	-29.899	20.967	0.055	0.742	0.245	0.988
N(2)-H(2A)	2.431	-47.953	-34.381	-32.303	18.731	0.064	0.742	0.228	0.969
	2.309	-39.774	-31.432	-29.771	21.429	0.056	0.740	0.248	0.989
	2.312	-40.468	-31.537	-29.899	20.967	0.055	0.245	0.742	0.988

^a Electron density ($e\text{\AA}^{-3}$)

^b Laplacian of Electron density ($e\text{\AA}^{-5}$)

^c Bond ellipticity

^d Hessian eigen values ($e\text{\AA}^{-5}$) and d_1 , d_2 are the distances in \AA between critical point and respective atoms of the bond in \AA

1st line indicates to HF method

2nd line indicates to B3LYP method

3rd line indicates to B3PW91 method

3.5 Atomic charges (AIM, MPA and NPA)

Partial atomic charges are real numbers describing the distribution of electron density in a molecule, thus providing clues as to the chemical behaviour of molecules. The approach of charges began to be used in physical chemistry and organic chemistry [37]. The partial atomic charges cannot be determined experimentally or derived straight forwardly from the results of quantum mechanics and many different methods have been developed for their calculation. The most common method for charge calculation is an application of the quantum mechanics approach and afterwards the utilisation of a charge calculation scheme.

In earlier, the balance of charges in different constellations of elements acts as a driving force for structural organization [38]. This infers also that charges will change when changing the structure [39, 40]. The atomic charges were calculated by a Bader analysis. The electrostatic interactions accurately calculated to the atomic charges of the molecule with various methods such as Mulliken Population Analysis (MPA), Natural Population Analysis (NPA) and Atoms in Molecules (AIM) charges. In the present research study of atomic charges, we have analysed the atomic charges of the molecule by AIM charges, MPA charges and NPA charges respectively.

The most important AIM charges of Quinacridone OLED molecule, all the C-atoms are found to be a positive and negative value for HF method. In this method, the C-atoms are increases from -0.020 e to 1.190 e. The DFT study of B3LYP methods of all C-atoms have been increasing values. These value increases from -0.030 e to 0.960 e. Similarly, the optimized methods of (B3PW91) of C-atom values are increases from -0.040 e to 0.970 e respectively (Table-4). The maximum observed variation for all methods of C-atoms are ~ 1.170 e. The N-atoms are only negative value for all the optimized methods. These values are increasing from -1.160 e to -1.500 e. Extremely, the O-atoms are same (negative) value for all the optimized methods (HF, B3LYP and B3PW91). The O-atoms are found to be unequal (-1.110 e to -1.320 e). The maximum observed variations are ~ 0.21 e.

By using HF method, MPA atomic charges of all C- atoms are varying from -0.319 e to 0.600 e. Another two methods of optimized, the variation of C-atoms are increases from -0.250 e to 0.395 e for (B3LYP); for B3PW91 method increases from -0.281 e to 0.447 e respectively. Similarly, the N-atoms regions are almost negative value for all the optimized methods. These variations are (negative value) increases from -0.547 e to -0.701 e respectively. However, the O-atom in the Quinacridone molecule is almost negative value for all the optimized methods are calculated and tabulated (Table-5). The calculated values are increases from -0.335 e to -0.454 e. The maximum observed variation for O-atoms are ~ 0.105 e. The NPA atomic charges of the Quinacridone molecule



of all C-atoms are found to be positive and negative values for all optimized methods; the NPA charges of all C-atoms values are increased from -0.271 e to 0.662 e. However, the N-atoms (negative value) in the three optimized methods are found to be unequal (-0.534 e to -0.621 e). The maximum observed variations in N-atoms are ~0.087 e. Particularly, the O-atoms in the all optimized methods (HF, B3LYP and B3PW91) are (negative value) increases from -0.591 e to -0.676 e [41]. The maximum observed variation in O-atoms are ~0.087 e. All the values are calculated and tabulated (Table-6).

Table 4. AIM charge of Quinacridone molecule.

Atoms	HF/ 6-311G**	B3LYP/ 6-311G**	B3PW91/ 6-311G**
C(1)	0.020	0.000	-0.010
C(2)	0.050	-0.010	-0.020
C(3)	0.480	0.400	0.420
C(4)	-0.010	-0.030	-0.040
C(5)	0.020	0.000	-0.010
C(6)	0.050	-0.010	-0.020
N(1)	-1.500	-1.160	-1.200
C(7)	0.470	0.390	0.410
C(8)	-0.020	-0.020	-0.030
C(9)	1.190	0.960	0.970
C(10)	0.060	0.000	-0.010
C(11)	-0.020	-0.020	-0.030
C(12)	0.470	0.390	0.410
C(13)	0.060	0.000	-0.010
C(14)	1.190	0.960	0.970
C(15)	-0.010	-0.030	-0.040
C(16)	0.480	0.400	0.420
N(2)	-1.500	-1.160	-1.200
C(17)	0.020	0.000	-0.010
C(18)	0.050	-0.010	-0.020
C(19)	0.020	0.000	-0.010
C(20)	0.050	-0.010	-0.020
O(1)	-1.320	-1.110	-1.120
O(2)	-1.320	-1.110	-1.120
H(1)	0.000	0.030	0.040
H(1A)	0.430	0.390	0.400
H(2)	-0.020	0.010	0.020
H(2A)	0.430	0.390	0.400
H(5)	0.050	0.070	0.080
H(6)	-0.010	0.020	0.030
H(10)	0.050	0.060	0.080
H(13)	0.050	0.060	0.080



H(17)	0.050	0.070	0.080
H(18)	-0.010	0.020	0.030
H(19)	0.000	0.030	0.040
H(20)	-0.020	0.010	0.020

Table.5. MPA charge of Quinacridone molecule.

Atoms	HF/ 6-311G**	B3LYP/ 6-311G**	B3PW91/ 6-311G**
C(1)	-0.050	-0.081	-0.089
C(2)	-0.127	-0.090	-0.098
C(3)	0.353	0.277	0.302
C(4)	-0.319	-0.250	-0.281
C(5)	-0.006	-0.024	-0.027
C(6)	-0.117	-0.092	-0.102
N(1)	-0.701	-0.547	-0.611
C(7)	0.351	0.287	0.315
C(8)	-0.277	-0.246	-0.274
C(9)	0.600	0.395	0.447
C(10)	-0.036	-0.025	-0.027
C(11)	-0.277	-0.246	-0.274
C(12)	0.351	0.287	0.315
C(13)	-0.036	-0.025	-0.027
C(14)	0.600	0.395	0.447
C(15)	-0.319	-0.250	-0.281
C(16)	0.353	0.277	0.302
N(2)	-0.701	-0.547	-0.611
C(17)	-0.006	-0.024	-0.027
C(18)	-0.117	-0.092	-0.102
C(19)	-0.050	-0.081	-0.089
C(20)	-0.127	-0.090	-0.098
O(1)	-0.454	-0.335	-0.349
O(2)	-0.454	-0.335	-0.349
H(1)	0.106	0.100	0.110
H(1A)	0.245	0.232	0.243
H(2)	0.094	0.092	0.103
H(2A)	0.245	0.232	0.243
H(5)	0.120	0.106	0.116
H(6)	0.102	0.099	0.109
H(10)	0.115	0.102	0.113
H(13)	0.115	0.102	0.113



H(17)	0.120	0.106	0.116
H(18)	0.102	0.099	0.109
H(19)	0.106	0.100	0.110
H(20)	0.094	0.092	0.103

Table. 6. NPA charge of Quinacridone molecule.

Atoms	HF/ 6-311G**	B3LYP/ 6-311G**	B3PW91/ 6-311G**
C(1)	-0.096	-0.157	-0.161
C(2)	-0.271	-0.243	-0.248
C(3)	0.292	0.210	0.206
C(4)	-0.252	-0.174	-0.177
C(5)	-0.072	-0.130	-0.135
C(6)	-0.254	-0.227	-0.232
N(1)	-0.621	-0.538	-0.534
C(7)	0.219	0.183	0.179
C(8)	-0.155	-0.126	-0.129
C(9)	0.662	0.520	0.516
C(10)	-0.165	-0.182	-0.186
C(11)	-0.155	-0.126	-0.129
C(12)	0.219	0.183	0.179
C(13)	-0.165	-0.182	-0.186
C(14)	0.662	0.520	0.516
C(15)	-0.252	-0.174	-0.177
C(16)	0.292	0.210	0.206
N(2)	-0.621	-0.538	-0.534
C(17)	-0.072	-0.130	-0.135
C(18)	-0.254	-0.227	-0.232
C(19)	-0.096	-0.157	-0.161
C(20)	-0.271	-0.243	-0.248
O(1)	-0.676	-0.596	-0.591
O(2)	-0.676	-0.596	-0.591
H(1)	0.188	0.204	0.209
H(1A)	0.392	0.395	0.399
H(2)	0.190	0.202	0.207
H(2A)	0.392	0.395	0.399
H(5)	0.211	0.225	0.231
H(6)	0.193	0.206	0.211
H(10)	0.217	0.228	0.234
H(13)	0.217	0.228	0.234

H(17)	0.211	0.225	0.231
H(18)	0.193	0.206	0.211
H(19)	0.188	0.204	0.209
H(20)	0.190	0.202	0.207

4. FRONTIER MOLECULAR ORBITAL AND THEIR ENERGIES

The Quinacridone OLED molecule obtain the one-electron wave function at the highest occupied molecular orbital (HOMO) and lowest unoccupied molecular orbital (LUMO) levels are analysed. The spatial distribution of the frontier orbitals plays an important role to reliably estimate image driven shifts of the relevant MO-energies [42]. The several ways of excitation energy of the Quinacridone molecule for different optimized methods (HF, B3LYP and B3PW91) are calculated. The Molecular Orbital energy level of Quinacridone molecule for HF, B3LYP and B3PW91 methods are represented in Fig.6. This shows that, the red color indicates the positive phase while the green color indicates the negative phase. Notably, the HF methods are calculated and the energy value is 8.49 eV. Likewise, the B3LYP and B3PW91 methods are calculated HLG values are 3.13 eV and 3.12 eV respectively (Table-7). The B3LYP and B3PW91 methods of the calculated values are very low with compared to HF methods. These values are almost matched with the experimental values are reported [43]. This lowest values indicating that electron and hole can be easily combined, and therefore its charge mobility performance would be the most improved through the molecule. The HLG values are almost equal to the energy gap obtained from density of states (DOS) spectrum. Fig.7 (a)-(c) shows the density of states spectrum of Quinacridone molecule with different optimized levels. Notably, the hybridization of the molecular lower level broadens the DOS peaks of the molecule. In the present study of molecules are mostly electron conductivity of the HLG may facilitate a large conduction through the Quinacridone OLED molecule.

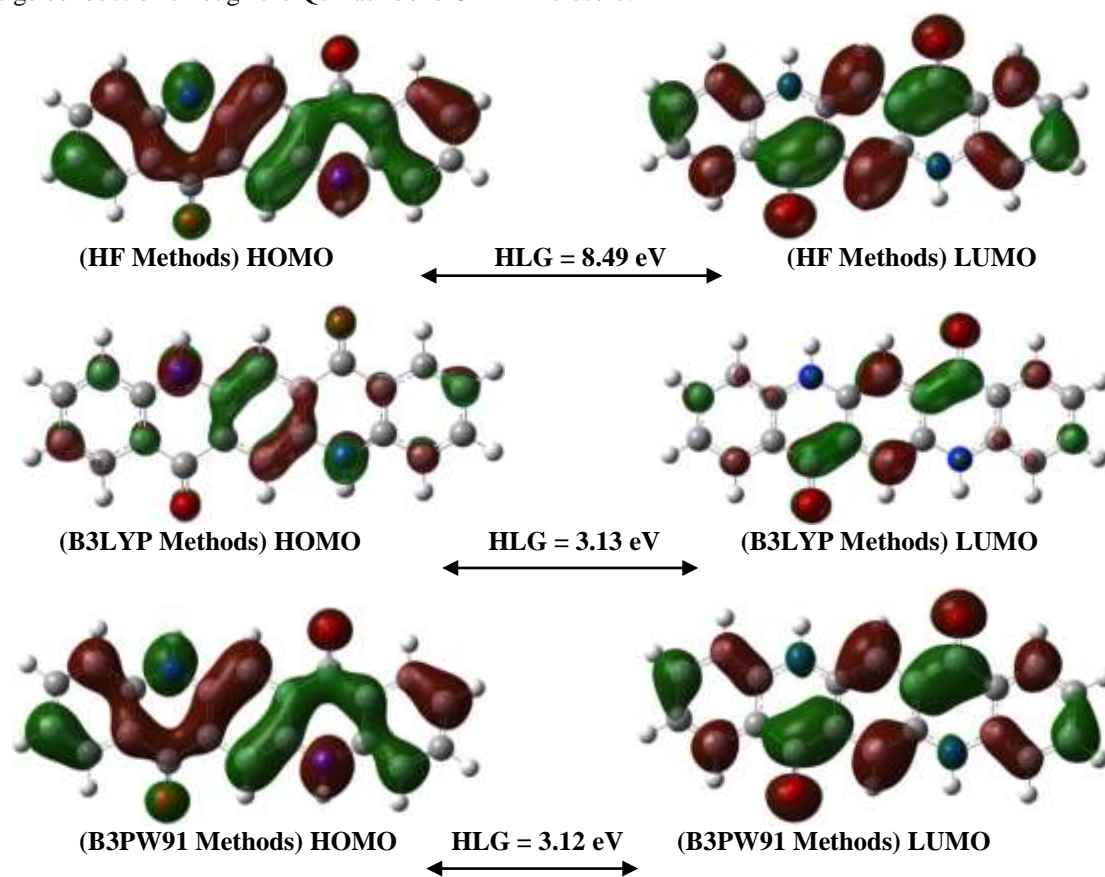
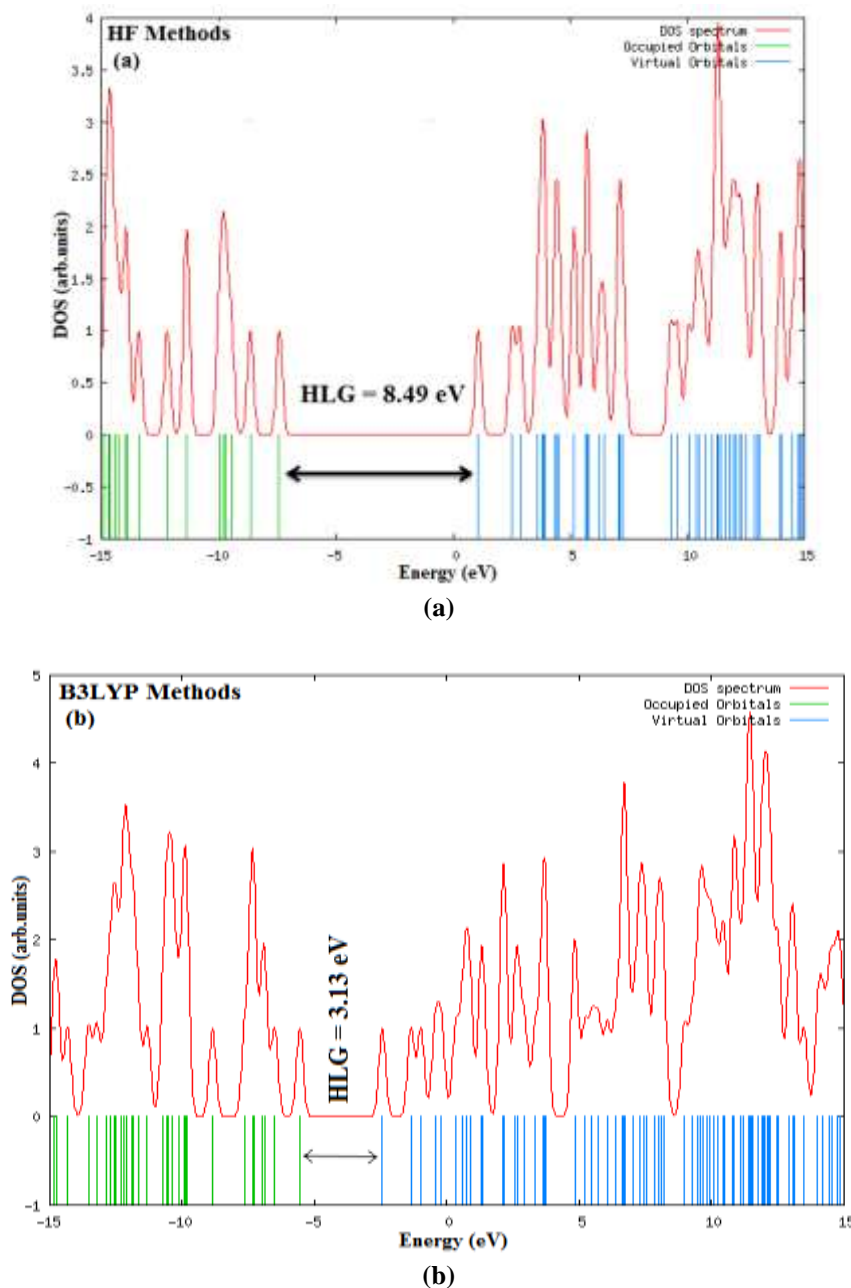


Figure.6. Shows the MO energy level diagrams of Quinacridone molecule at HF, B3LYP and B3PW91 methods. Red color: Positive Phase; Green color: Negative Phase

Table.7. Frontier of molecular orbital energies of Quinacridone molecule.

Methods	HOMO	LUMO	HLG (eV)
HF	1.08	-7.41	8.49
B3LYP	-2.43	-5.56	3.13
B3PW91	-2.51	-5.63	3.12



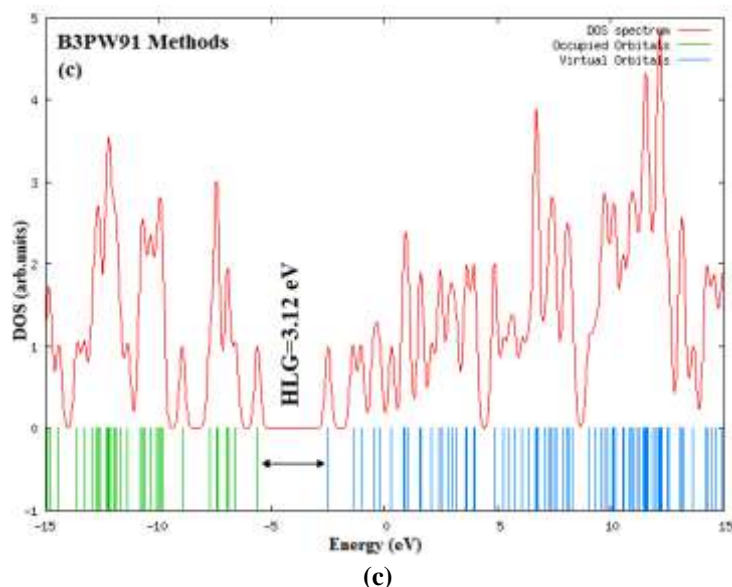
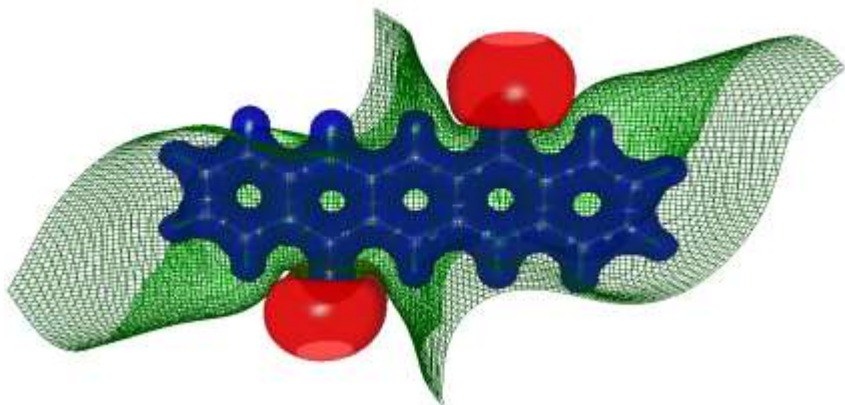


Figure.7 (a)-(c) Depicts the density of states (DOS) for Quinacridone OLED molecule at HF, B3LYP and B3PW91 methods. Green line indicates HOMO; Blue line indicates LUMO.

4.1. Molecular Electrostatic Potential

The very important applications of my research articles, it is used to identify the charged region of the Quinacridone has been calculated to electrostatic potential and classified to the strong electronegative and positive regions appear in the molecule. The molecular electrostatic potential (MESP) depicts the electronic density and gives the information regarding electrophilic, nucleophilic attack as well as hydrogen–bonding interactions [44]. Fig.8 (a)-(c) represents the Molecular Electrostatic Potential (MESP) obtained from different optimized energy levels (HF, B3LYP and B3PW91). It shows that both negative (red) and positive (blue) electrostatic potential regions of the molecule, drawn at isosurface values $\pm 0.5 \text{ e}\text{\AA}^{-1}$ [45]. In the present research study, the C and N atoms indicates the strongest attraction and the O-atoms indicate the strongest repulsion. The negative electrostatic potential is concentrated entirely around the O-atoms; whereas in the rest of the positive ESP regions at low energy level of the molecules. This charged region changes effective from the negative potential appears around the O atoms. This difference is change to the group charge effect of the molecule. The electrostatic potential also calculated to the polarization of electron correlation and the charge transfer to the molecule.

Methods	Molecular Electrostatic Potential
HF/ 311G**	 <p>Fig.(a)</p>

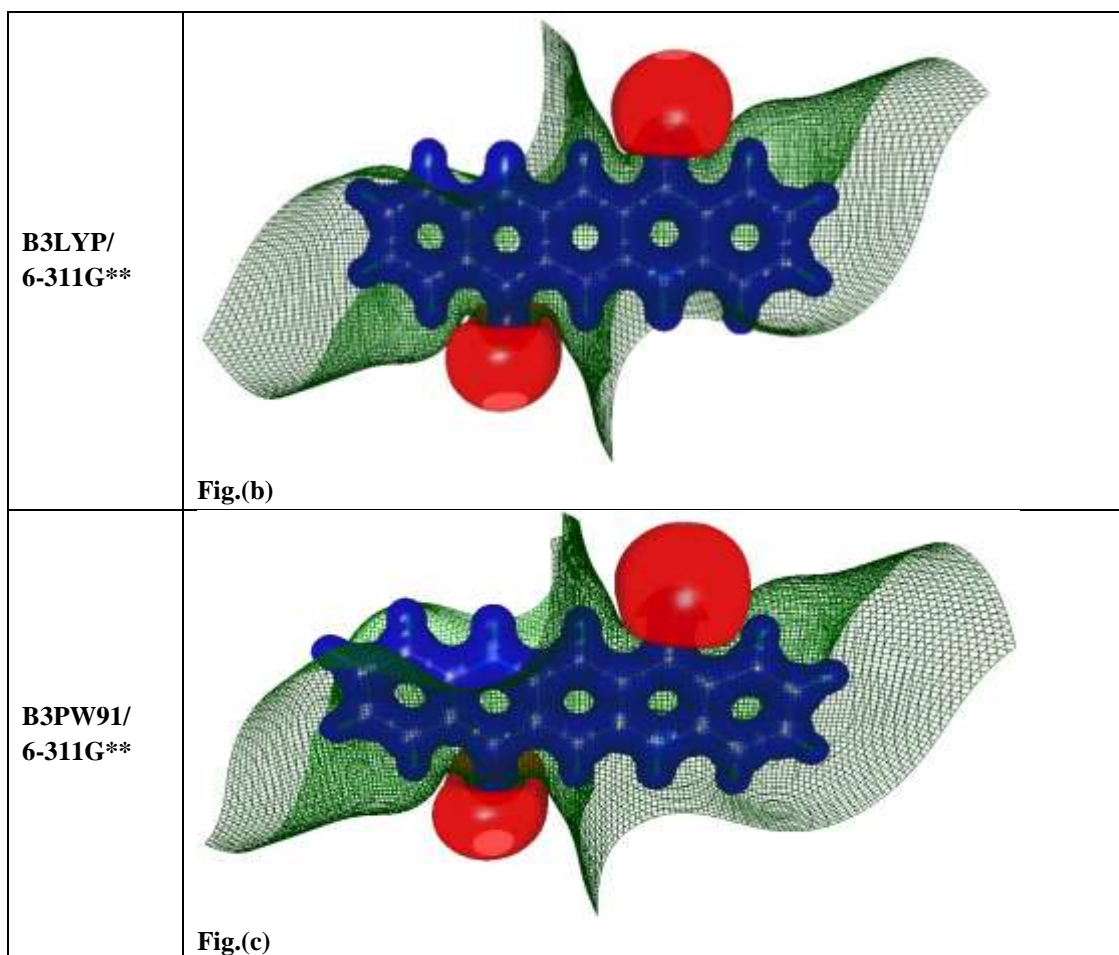


Figure. 8 (a)-(c). Molecular electrostatic potential of Quinacridone molecule at HF, B3LYP and B3PW91 methods. Blue: positive potential ($0.05 \text{ e}\text{\AA}^{-1}$), Red: negative potential ($-0.05 \text{ e}\text{\AA}^{-1}$), Green: neutral Potential ($0.00 \text{ e}\text{\AA}^{-1}$).

5. CONCLUSION

In this perspective, the basic theory and applications of quantum theory of atoms in molecules have been presented. The present investigation of research articles, the electron transport properties of Quinacridone OLED molecule are calculated from Density Functional Theory by using HF, B3LYP and B3PW91 basis sets to explore its structural aspects also compared. The HF method of these molecules are analysed the geometrical parameters and the electrostatic transport properties of the molecule has been premeditated and associated with other two optimized methods. The chemical aspects of the charge distribution are described in terms of Density deformation, Laplacian of total electron density as well as the electrostatic potential. The bond topological analysis distinguishes the charge distribution in C–C as well as N–C and O–C bonds Quinacridone OLED molecule. The HOMO-LUMO Gap of the molecule occur 8.94 eV, 3.13 eV and 3.12 eV for all the optimized methods respectively. The Large HOMO-LUMO Gap utilizing wide energy gap materials as the host to realize high efficient green emission of Quinacridone molecule. These results could be helpful in understanding the Quinacridone green dopant derivative molecule is high quantum efficiency, longer lifetime and simplifying the process of fabricating full color OLEDs. This research article may very useful to industrial organic pigment.

REFERENCES

1. Squires R, A.D. Lewis Adam A. Zaczek J and Timothy Korter M, (2017), Distinguishing Quinacridone Pigments via Terahertz Spectroscopy: Absorption Experiments and Solid-State Density Functional Theory Simulations, Journal of Physical Chemistry A, 121 (18): 3423-3429.



- Struve WS. (1958), US Patent 2. 844.485.
- Nameless. Studies in Quinacridone Chemistry. DuPont Innovation, 2: 14-17. Editorial office: DuPont Building, Wilmington, Delaware 19898, USA. (1970).
- Labana SS, Labana LL, (1967), Quinacridone. Chemical Reviews, 67 (1), 1-18.
- Weiping Chen, Kui Tian, Xiaoxian Song, Zuolun Zhang, Kaiqi Ye, Gui Yu and Yue Wang, (2015), Large π -Conjugated Quinacridone Derivatives: Syntheses, Characterizations, Emission, and Charge Transport Properties, Organic Letters, 17 (24), 6146–6149.
- Koezuka, H.; Tsumura, A.; Ando, T. (1987), "Field-effect transistor with polythiophene thin film". Synthetic Metals. 18 (1-3), 699–704.
- Kafafi Z. H, Murata H, Picciolo L.C, Mattoussi H, Merritt C.D, Iizumi Y, Kido J, (1999), Electroluminescent properties of functional Π -electron molecular systems, Pure Applied Chemistry, 71 (11), 2085-2094.
- Shaheen S.E, Kippelen B, Peyghambarian N, Wang J.F, Anderson J.D, Mash E.A, Lee P.A, Armstrong N.R, Kawabe Y., (1999), Energy and charge transfer in organic light-emitting diodes: A soluble quinacridone study, Journal of Applied Physics. 85 (11), 7939-7945.
- Tang C.W, VanSlyke S.A, Chen C.H, (1989), Electroluminescence of doped organic thin films, Journal of Applied Physics, 65 (9), 3610-3616.
- Shi J, Tang C.W, (1997), Doped organic electroluminescent devices with improved stability, Applied Physics Letter, 70 (13), 1665-1667.
- Kundu S, Fujihara K, Okada T, Matsumura M, (2000), Excitation Migration from Photoexcited Tris(8-hydroxyquinolino)aluminium to Quinacridone in Codeposited Thin Films, Japanese Journal of Applied Physics, 39, 5297.
- Hung L.S, Chen C.H, (2002), Recent progress of molecular organic electroluminescent materials and devices, Materials Science. Engineering, R: Reports, 39 (5-6), 143-222.
- Hamada Y, Sano T, Shibata K, Kuroko K, (1995), Influence of the Emission Site on the Running Durability of Organic Electroluminescent Devices, Japanese Journal of Applied Physics, 34 L824 – L826.
- Berggren M, Dodabalapur A, Slusher R.E, (1997), Applied Physics Letter, 71 (16), 2230-2232.
- Tsujimura T. OLED Display Fundamentals and Applications (Wiley Series in Display Technology). Wiley-VCH. (2012).
- Paulus E. F, Leusen F. J. J, and Schmidt M. U, (2007), "Crystal structures of quinacridone", Crystal Engineering Communications, 9, (2), 131–143.
- Lincke G, (2000), "A review of thirty years of research on quinacridone. X-ray crystallography and crystal engineering", Dyes and Pigments, 44, (2), 101–122.
- Mateusz Barczewski, Danuta Matykievicz, and Bart Bomiej Hoffmann, (2017), 'Effect of Quinacridone Pigments on Properties and Morphology of Injection Molded Isotactic Polypropylene' International Journal of Polymer Science, 2017, 1-8,
- Duan L, Hou L, Lee T.W, Qiao J, Zhang D, Dong G, Wang L, Qiu Y, (2010), Solution processable small molecules for organic light-emitting diodes, Journal of Material Chemistry, 20 (31), 6392-6407.
- Puschnig P, Reinisch E.M, Ules T, Koller G, Soubatch S, Ostler M, Romaner L, Tautz F. S, Ambrosch-Draxl C, and Ramsey M. G, (2011), 'Orbital tomography: Deconvoluting photoemission spectra of organic molecules' Physical Review, B 84, 235427.
- Seminario J.M, Politzer P, (1995), Molecular Density Functional theory: A tool for Chemistry, Elsevier, New York.
- Wadt W.R, Hay P.J, (1985), Journal of Chemical Physics, 284: 82.
- M.J. Frisch, G.W. Trucks, H.B. Schlegel, G.E. Scuseria, M.A. Robb, J.R. Cheeseman, J.A. Montgomery, Jr., T. Vreven, K.N. Kudin, J.C. Burant, J.M. Millam, S.S. Iyengar, J. Tomasi, V. Barone, B. Mennucci, M. Cossi, G. Scalmani, N. Rega, G.A. Petersson, H. Nakatsuji, M. Hada, M. Ehara, K. Toyota, R. Fukuda, J. Hasegawa, M. Ishida, T. Nakajima, Y. Honda, O. Kitao, H. Nakai, M. Klene, X. Li, J. E. Knox, H.P. Hratchian, J.B. Cross, C. Adamo, J. Jaramillo, R. Gomperts, R.E. Stratmann, O. Yazyev, A.J. Austin, R. Cammi, C. Pomelli, J.W. Ochterski, P.Y. Ayala, K. Morokuma, G.A. Voth, P. Salvador, J.J. Dannenberg, V.G. Zakrzewski, S. Dapprich, A.D. Daniels, M.C. Strain, O. Farkas, D.K. Malick, A.D. Rabuck, K. Raghavachari, J.B. Foresman, J.V. Ortiz, Q. Cui, A.G. Baboul, S. Clifford, J. Cioslowski, B.B. Stefanov, G.



- Liu, A. Liashenko, P. Piskorz, I. Komaromi, R.L. Martin, D.J. Fox, T. Keith, M.A. Al- Laham, C.Y. Peng, A. Nanayakkara, M. Challacombe, P.M.W. Gill, B. 47 Johnson, W. Chen, M.W. Wong, C. Gonzalez, and J.A. Pople, Gaussian Inc, P. A. Pittsburgh, (2003).
24. Schlegel B, (1982), Journal of Computational Chemistry, 3, 214.
 25. AIMAll (Version 10.03.25) Todd A. Keith (aim.tkgristmill.com), (2010).
 26. Tsirelson S.V, WinXPRO, (2002), A program for calculating crystal and molecular properties using multipole parameters of the electron density, Journal of Applied Crystallography, 35, 371–373.
 27. Frish A, Lecn E, Nielson A.B, Holder A, Roy Dennigton A.J, Keith T.A, Gaussian Incorporated, Pittsburgh PA, (2003).
 28. Boyle N.O, GaussSum, Revision 2.1, <http://GaussSum.sf.net>.
 29. Joseph, S. Comins, D. L. (2002), Current Opinion in Drug Discovery and Development, 5, 870.
 30. Schmidt R, (1965), Chemische Berichte, 98,334.
 31. Fisyuk A.S, Vorontsova M.A, and Ivanov S.A, (1994), Novel Synthesis of 5,6-dihydropyridin-4(3H)-one, Chemistry of Heterocyclic compounds, 30, (6)
 32. David Stephen A., Srinivasan P., Kumaradhas P., (2011), Bond Charge Depletion, Bond Strength and the Impact Sensitivity of High Energetic 1,3,5-Triamino-2,4,6-trinitrobenzene (TATB) Molecule: A Theoretical Charge Density Analysis, Comput. Theo. Chem., 967, 250-256.
 33. R.F.W. Bader, (1990), Atoms in Molecule; A Quantum theory, Clarendon Press, Oxford, UK.
 34. Popelier P.L.A, (1999), Atom in Molecules an Introduction, Pearson Edition, Harlow, UK.
 35. Seminario J. M and Politzer P, (1995), Molecular Density Functional Theory: A Tool for Chemistry, Elsevier, New York.
 36. Arputharaj David Stephen, Reji Thomas, Ponnusamy Srinivasan, Vijayan Narayanasamy, Poomani Kumaradhas, (2011), Exploring the bond topological and electrostatic properties of benzimidazole molecule via experimental and theoretical charge density study Journal of Molecular Structure, 989, 122–130.
 37. Dudek A.Z, Arodz T, Galvez J, (2006), Computational methods in developing quantitative structure-activity relationships (QSAR): a review. Comb Chem High Throughput Screen (3):213–228.
 38. Beck H.P, (2015), A DFT study on the correlation between topology and Bader charges: part I, effects of compression and expansion of As₂O₅, Solid State Sci. 41, 1-7.
 39. Beck H.P, (2015), A DFT study on the correlation between topology and Bader charges: part II, effects of compression and expansion of V₂O₅, Solid State Sci. 43, 1-8.
 40. Beck H.P, (2015), A study on AB₂O₆ compounds, part V: a DFT study on charge balance as driving force for structural organization, Z. Krist. 7, 449 – 458.
 41. Reed, A.E., R.B. Weinstock, and F. Weinhold, (1985), Natural population analysis, The Journal of Chemical Physics, 83(2), 735-746.
 42. Slattey D. K, Linkous C. A, Gruhn N. E, and Baum J, (2001), Dyes Pigments, 49, 21.
 43. Daniel Luftner, Sivan Refaely-Abramson, Michael Pachler, Roland Resel, Michael G. Ramsey, Leor Kronik, and Peter Puschnig, (2014), Experimental and theoretical electronic structure of quinacridone, PHYSICAL REVIEW B 90, 075204-1-10.
 44. Prasad M.V.S, Chaitanya K, Udaya Sri N, Veeraiah V, (2013), Experimental and theoretical (HOMO, LUMO, NBO analysis and NLO properties) study of 7-hydroxy-4-phenylcoumarin and 5,7-dihydroxy-4-phenylcoumarin Journal of Molecular Structure 1047, 216–228.
 45. Subramanian Palanisamy, Ponnusamy Srinivasan, Aruptharaj David Stephen and Karuppannan Selvaraju, (2018), Charge Density and Electrical Characteristics of 1,2-di([1,1'-biphenyl]-4-yl)ethyne (DBPE) Molecular Nanowire by Quantum Chemical Study, Journal of Computational Theoretical Nanoscience, Vol. 15, No. 5, 1516–1527.

Cite this Article: S. Palanisamy, P. Srinivasan, A. David Stephen, B. Jothi, K. Selvaraju (2023). Theoretical Investigation on Highly Efficient Quinacridone Derivatives for Green Dopant OLEDs: A DFT Simulation. International Journal of Current Science Research and Review, 6(7), 4836-4858